

Improved rate for the oxygen reduction reaction in sulfuric acid electrolyte by Pt(111) surface modified with melamine

Milena Zorko^{1,2}, Pedro Farinazzo Bergamo Dias Martins¹, Justin G. Connell¹, Pietro Papa Lopes¹, Ne-nad M. Markovic¹, Vojislav R. Stamenkovic¹, Dusan Strmcnik¹ *

¹Materials Science Division, Argonne National Laboratory, Lemont, IL 60439, USA

²Centre of Excellence for Low-Carbon Technologies (CoE LCT), Hajdrihova 19, 1000 Ljubljana, Slovenia

KEYWORDS: oxygen reduction reaction; platinum; anion adsorption; melamine; electrocatalysis; fuel cells.

ABSTRACT: The feasible commercialization of alkaline, phosphoric acid and polymer electrolyte membrane fuel cells depends on the development of oxygen reduction reaction (ORR) electrocatalysts with improved activity, stability, and selectivity. The rational design of surfaces to ensure these improved ORR catalytic requirements rely on so-called ‘descriptors’ (e.g., the role of covalent and non-covalent interactions on platinum surface active sites for ORR). Here, we demonstrate that through the molecular adsorption of melamine onto the Pt(111) surface [Pt(111)-M_{ad}], the activity can be improved by a factor of 20 compared to bare Pt(111) for the ORR in a strongly adsorbing sulfuric acid solution. The M_{ad} moieties act as ‘surface blocking bodies’, selectively hindering the adsorption of (bi)sulfate anions [well-known poisoning spectator of the Pt(111) active sites] while the ORR is unhindered. This modified surface is further demonstrated to exhibit improved chemical stability relative to Pt(111) patterned with cyanide species (CN_{ad}), previously shown by our group to have a similar ORR activity increase compared to the bare Pt(111) in sulfuric acid electrolyte, with Pt(111)-M_{ad} retaining a >9-fold higher ORR activity relative to bare Pt(111) after extensive potential cycling as compared to a >3-fold higher activity retained on CN_{ad}-covered Pt(111) surface. We suggest that the higher stability of Pt(111)-M_{ad} interface stems from melamine’s ability to form intermolecular hydrogen bonds, which effectively turns the melamine molecules into larger macromolecular entities with multiple anchoring sites and thus more difficult to remove.

INTRODUCTION

The development of alkaline, polymer electrolyte membrane and phosphoric acid fuel cells has advanced astonishingly in the past two decades. One of the reasons is the continuous design of new active materials for electrocatalysis of the kinetically sluggish and complicated oxygen reduction reaction (ORR), known as one of the major obstacles for the reliable commercialization of fuel cells. Among these designed materials, platinum-based surfaces continue to be the most active and durable catalysts for the reduction of O₂ - particularly in acidic media - due to their superior chemical stability over non-noble transition metal surfaces. Traditionally, the parameters considered as guidelines to improve platinum ORR electrocatalysis are based on fine-tuning of the platinum electronic and structural surface properties, which have been shown to potentially increase its catalytic performance¹⁻⁵. Although the number of approaches used for ‘surface-tuning’ is enormous, platinum alloying with non-noble transition metals and/or tailoring platinum nanoparticles with preferential facets have been the most commonly used methods³⁻⁷. More recently, however, precise control of the components and structure of the electrified interface between the platinum electrode surface and the electrolyte (solid/liquid interface) has also been established as a promising way for improvement of the rate of various electrochemical reactions (e.g., oxygen and hydrogen oxidation/reduction reactions)⁸⁻¹⁰. For instance, our group demonstrated the influence of non-covalent interactions (i.e., weaker electrostatic interactions that include ion-dipole, hydrogen bonding and van der Waals interactions,

usually between surface adsorbates and ions/molecules in the interfacial region) on the kinetic rate of the hydrogen oxidation, oxygen reduction, and methanol oxidation reactions on platinum surfaces in alkaline media⁹, providing evidence that at high pH values, the nature and concentration of dissolved cations also play a role as ‘modulating parameters’ for enhancing electrocatalytic activity. On the other hand, the kinetic activity of the electrochemical interface can also be affected by covalently-bonded species¹¹ (i.e., adsorbates that form strong bonds through electron sharing with the surface atoms). A familiar example is the adverse effect the adsorption of (bi)sulfate (HSO₄⁻ and SO₄²⁻), phosphate (PO₄³⁻) and/or hydroxyl (OH_{ad}) species have on platinum active sites for the ORR¹². While the adsorption of ‘small’ OH_{ad} species on Pt in aqueous electrolytes is hard to prevent without changing the electronic structure of the metal, there are alternate routes for preventing the adsorption of ‘bulky’ (bi)sulfate or phosphate species. One approach is the chemical modification of electrode surfaces with covalently-bonded foreign species, which can affect the reaction kinetics by participating directly in a cooperative process (called the ‘bi-functional process’), or indirectly as surface-blocking spectators (known as the ‘third-body’ effect^{13,14,15}). In one such attempt, we modified a single-crystalline Pt(111) surface through the adsorption of cyanide molecules [Pt(111)-CN_{ad}] and monitored the influence of this molecular modifier on the ORR rate in different electrolytes⁸. We observed an unprecedented ORR activity increase on Pt(111)-CN_{ad} compared to the bare Pt(111) in electrolytes containing sulfate/phosphate anions (a 25-/10-

fold activity enhancement, respectively). Furthermore, no appreciable difference was seen in the presence of perchlorate anions (well-known weakly adsorbing anion¹²). These experimental facts guided us towards the conclusion that CN_{ad} moieties indeed have an appreciable influence on ORR electrocatalysis through a third-body effect, effectively impeding the undesired adsorption of poisonous species (SO₄²⁻ and PO₄³⁻), while not affecting the overall oxygen reduction mechanism⁸.

A common weakness of the modified electrode surfaces is their (electro)-chemical stability. This is not surprising if we consider that the monolayer or sub-monolayer amount of the spectator must compete against several species (e.g., anions and water molecules) present in the electrolyte in the millimolar to molar concentration range and hence the stability of anion-modifiers will depend on the strength of their interaction with the electrocatalyst surface. To achieve that, we can use molecules that form a stronger bond with the surface or use molecules that bond with multiple bonds, i.e. a “multi-dentate” anchoring, thus achieving a collectively stronger adsorption to the surface. One molecule that could fit this description is melamine. Melamine is a heterocyclic aromatic molecule composed of a triazine ring (C₃N₃) and one amine group (-NH₂) bonded on each of the carbon atoms from the aromatic ring. It has been shown that the preparation of melamine-adsorbed on various surfaces [e.g., Au(111)¹⁶, Cu(111)¹⁷, Ni(111)¹⁸, and Pd(111)¹⁹] and highly oriented pyrolytic graphite (HOPG)²⁰ surface is relatively simple and presented straightforward reproducibility, exhibiting well-ordered patterns witnessed by scanning tunneling microscopy (STM). Moreover, the metal-melamine moieties showed remarkable stability under UHV at different temperatures. However, the electrocatalytic performance of these metal-melamine interfaces has seldomly been explored^{21,22}.

In this manuscript, we deposited a melamine adlayer on Pt(111) surface [Pt(111)-M_{ad}] following the concept adopted and improved by our research group, i.e. electrocatalyst surface modification by foreign chemical species^{8,23-25}, and test the ability of this interface to selectively block larger anions from poisoning the surface, while allowing ORR to proceed unhindered. Sulfuric acid was chosen as the acidic media with the well-known strongly adsorbing anions, i.e. (bi)sulfate species. The preparation method is simple and presents high reproducibility. The ORR activity of Pt(111)-M_{ad} is similar to the Pt(111) surface adsorbed with cyanide species [Pt(111)-CN_{ad}] in sulfuric acid solution [>20-fold increase compared to the bare Pt(111)]. The kinetic rate increase is attributed to the M_{ad} moieties ability to suppress the poisonous adsorption of (bi)sulfate anions on platinum surface active sites, an effect also observed for CN_{ad} moieties⁸. Moreover, Pt(111)-M_{ad} showed much greater stability than Pt(111)-CN_{ad}, which is attributed to the hydrogen-bonded melamine networks (absent in the CN_{ad} adlayer), which act as a stability promoter of the Pt(111)-M_{ad} surface during ORR.

EXPERIMENTAL

All electrochemical measurements were done in 0.05 M sulfuric acid solutions prepared with ultra-pure deionized water (R \geq 18.2 MΩ cm, Milli-Q system) and ultra-high purity H₂SO₄ (OmniTrace Ultra, EMD). The electrolyte temperature was \sim 293 K, purged either with argon gas (99.9999% purity, Airgas) for cyclic voltammetry (CV) or oxygen gas (99.999% purity, Airgas) for oxygen reduction reaction (ORR) polarization curves, and the potential sweep rate was 50 mV s⁻¹ for all curves

presented in this work. A platinum wire (99.997% purity, Alfa Aesar) and a silver/silver chloride electrode saturated with potassium chloride (BASi) were used as the counter and reference electrodes, respectively, although all potentials presented hereafter are showed versus the reversible hydrogen electrode (RHE), whose potential was determined in a separated experiment using the same electrochemical conditions mentioned above except the electrolyte was purged with hydrogen gas (99.9999% purity, Airgas). The preparation of the single-crystalline platinum surface, Pt(111), was done as described in previous work²⁶. Briefly, a 6 mm surface diameter by 4 mm height Pt(111) disc (Princeton Scientific) was annealed in a controlled atmosphere of hydrogen/argon gas mixture (3%H₂/97%Ar mixture, Airgas) at \sim 1 atm and \sim 1,473 K for 7 min with the help of a radio frequency induction system (EASYHeat, Ambrell), and cooled slowly (ca. 7 min) in the same atmosphere conditions. The Pt(111) surface was protected with water droplet before being exposed to the laboratory atmosphere. The platinum disc was then carefully assembled into a rotating disc electrode (RDE) configuration to avoid exposure of Pt(111) surface to air [a polypropylene thin sheet was used to support the platinum disc during the RDE assembling, with the Pt(111) surface facing towards the sheet protected with a thin water film]. The RDE system was then attached to a shaft and connected to a rotator machine (MSR, Pine Research). The Pt(111) surface was immersed in the electrolyte at controlled potential (E = 0.45 V) before the electrochemical experiments. A rotation speed of 1,600 r.p.m. was used to obtain the ORR polarization curves (CVs were obtained without rotation). All ORR polarization curves showed in this work are the positive-going potential sweep (‘anodic sweep’).

Two slightly different approaches were used to prepare the cyanide and melamine adlayers on Pt(111) surface. First, for the preparation of the cyanide adlayer [Pt(111)-CN_{ad}] we immersed the fresh-annealed Pt(111) surface (protected with a droplet of water) in a 0.1 M potassium cyanide (\geq 97.0% purity, Aldrich) solution for ca. 25 min⁸. The platinum crystal was rinsed thoroughly with water before being assembled into RDE configuration. Five CVs (0.05 V $<$ E $<$ 0.95 V) were performed to remove any residual excess of cyanide species from the platinum surface. Second, for the preparation of the melamine adlayer [Pt(111)-M_{ad}] we added 50 μL of a hot (\sim 343 K) 50 μM melamine (99% purity, Aldrich) solution on a fresh-annealed Pt(111) surface (protected with a film of water) already assembled in the RDE configuration. The melamine solution droplet was evaporated from the platinum surface under vacuum and controlled temperature (ca. 303 K). Finally, the Pt(111)-M_{ad} surface was rinsed thoroughly with water. Similar to bare Pt(111) surface, the modified Pt(111) surfaces were immersed in the electrolyte at E = 0.45 V.

In order to probe the presence of adsorbed melamine on the platinum surface, we performed X-ray photoelectron spectroscopy (XPS) on Pt(111) and Pt(111)-M_{ad} surfaces. The bare and modified Pt(111) surfaces were prepared exactly in the same fashion as for the electrochemical studies, subsequently transferred to an antechamber protected by a water droplet later evaporated under vacuum before transfer to the main glovebox chamber (O₂ and H₂O: < 0.5 ppm), which is connected to a load lock ultra-high vacuum (UHV) chamber before its transfer to the position for XPS analysis. XPS measurements were performed using a Specs PHOIBOS 150 hemispherical energy analyzer with a monochromatic Al K α X-ray source. The survey spectra were measured using a pass energy of 40 eV at a

resolution of 0.2 eV step⁻¹ and a total integration time of 0.1 s point⁻¹. The core level spectra were measured using a pass energy of 20 eV at a resolution of 0.05 eV step⁻¹ and a total integration time of 0.5 s point⁻¹. Deconvolution was performed using CasaXPS software²⁷ with a Shirley-type background and 70-30 Gaussian-Lorentzian peak shapes. Charge referencing was performed using adventitious carbon at 284.8 eV. Pt(111)-CN_{ad} was not characterized by XPS due to the vast past exploration and reproducibility of this surface found in the literature²⁸⁻³⁹.

RESULTS AND DISCUSSION

We begin our analysis by interpreting the cyclic voltammograms (CVs) of the bare Pt(111), and Pt(111) with cyanide or melamine adlayers [hereafter denoted as Pt(111), Pt(111)-CN_{ad}, and Pt(111)-M_{ad}, respectively] in 0.05 M H₂SO₄ (Fig. 1a). The well-known potential interval regions of Pt(111) CV in sulfuric acid is evident: region I, adsorption of hydrogen, known as underpotential deposited hydrogen region ($H^+ + e^- \rightleftharpoons H_{upd}$), located between 0.05 - 0.4 V, region II, located between 0.4 - 0.6 V, where the adsorption of (bi)sulfate anions is considered to take place, followed by region III, 0.6 - 1.0 V, where the adsorption of OH_{ad} and the formation of platinum oxide (PtO) are observed^{8,12,40,41}.

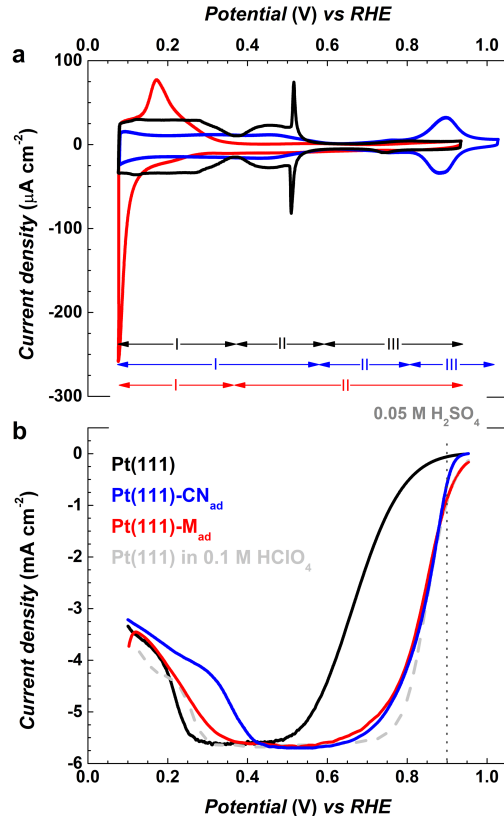


Figure 1. Characteristic cyclic voltammetry profiles for the bare and modified Pt(111) surfaces and their respective polarization curves for oxygen reduction reaction (ORR). a, Cyclic voltammograms for the bare (black curve), CN_{ad}- (blue curve), and M_{ad}-covered (red curve) Pt(111) surface; b, their corresponding ORR polarization curves (positive-going potential sweep). The curves were measured in a, argon-, and b, O₂-saturated 0.05 M sulfuric acid solutions (~293 K), at sweep rate of 50 mV s⁻¹. The ORR polarization curves were recorded at 1,600 r.p.m. using the rotating disc electrode configuration. The bare Pt(111) ORR polarization

curve recorded in 0.1 M perchloric acid solution (gray dashed curve) is shown for comparison in b. A dotted-vertical line present in b serves as an eye-guide to spot the difference in ORR activities (E = 0.9 V) between the bare and modified Pt(111) surfaces. The regions I, II, and III showed in a represent the H_{upd} adsorption, (bi)sulfate adsorption, and OH_{ad} adsorption, respectively.

Although the Pt(111)-CN_{ad} CV potential regions I, II, and III are expanded/contracted compared to Pt(111) (Fig. 1a), virtually all the same qualitatively features are present, namely: region I, 0.05 - 0.6 V, the H_{upd} region, followed by a small pseudocapacitance region between 0.6 - 0.8 V (region II), and finally the region III, 0.8 - 1.0 V, where the formation of platinum oxygenated species takes place. It's important to notice the presence of a small but distinguishable current density between ~0.7 - ~0.8 V, which is assigned to the adsorption/desorption of a tiny amount of (bi)sulfate species onto the Pt(111) surface⁸. Nevertheless, the site availability for 'bulky' (bi)sulfate adsorption is incredibly small (region II, Fig. 1a), compared to the site availability for 'small' O₂ molecule adsorption. As previously described, the CN_{ad} ensemble on Pt(111) surface acts as a 'blocking body' ('third-body' effect^{13,14}), sterically hindering the specific adsorption of (bi)sulfate anions on platinum surface sites⁸. In contrast, the adsorption of oxygen molecules (necessary for ORR electrocatalysis) is possible in the vicinity of adsorbed CN_{ad}, i.e. free Pt(111) surface sites, resulting in an astonishing improvement of ORR activity (e.g., 25-fold increase versus the bare platinum in sulfuric acid electrolyte)⁸.

Fig. 1a also includes the Pt(111)-M_{ad} CV in aqueous sulfuric acid electrolyte, which shows two potential regions: region I, 0.05 - 0.4 V, assigned to the adsorption of hydrogen (H_{upd}). Here we note the asymmetry in the anodic and cathodic H_{upd} peaks, which we speculate stems from slow rearrangement and/or re-orientation of melamine molecules while always staying attached to the surface. Region II, 0.4 - 1.0 V, is fairly featureless and reminiscent of typical double layer charging. However, the currents in this region are higher than those typically observed for double layer charging, suggesting that some adsorption processes do indeed occur at these potentials as well. Nevertheless, it is clear that the adsorption of (bi)sulfate is definitively suppressed on Pt(111)-M_{ad} surface in the same fashion as on Pt(111)-CN_{ad} - likely via the same 'third-body' effect. Region III - observed for the bare and CN_{ad}-covered platinum surfaces - is absent in the Pt(111)-M_{ad} CV profile, indicating that the adsorption of oxygenated species (e.g., OH_{ad}) is completely suppressed on this electrocatalyst surface in the potential window measured for this work. As will be discussed later, this characteristic has a strong impact on the ORR kinetics (Fig. 1b).

To verify the chemical integrity of the melamine adlayer on Pt(111), we performed X-ray photoelectron spectroscopy (XPS) analysis of unmodified Pt(111) and Pt(111)-M_{ad} surfaces. The surface preparation procedure was done identically as for the electrochemical measurements. Fig. 2 summarizes the XPS survey, nitrogen 1s and carbon 1s core level spectra obtained for both electrocatalyst surfaces. The platinum peaks shown in the survey spectra are remarkably similar, implying that the platinum surface remains virtually intact even after the melamine assembling. Moreover, the fact that the platinum peaks show a zero-oxidation state surface (metallic platinum) indicates our method for crystal surface preparation does not introduce foreign impurities which may induce platinum surface oxidation (note also the absence of undesirable elements in the survey).

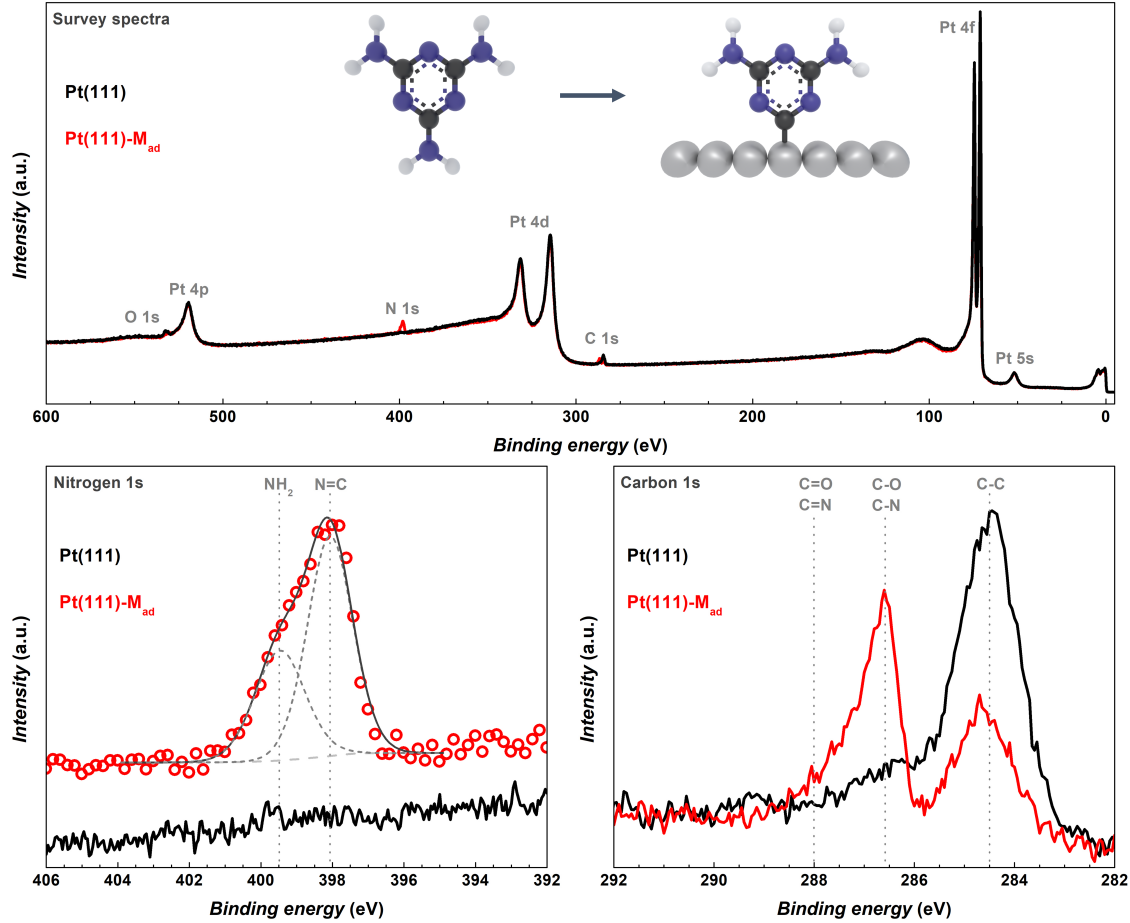


Figure 2. Chemical characterization of the bare and melamine-modified Pt(111) surfaces by X-ray photoelectron spectroscopy (XPS). The survey spectra (top) for bare (black curve) and melamine-covered (red curve) Pt(111) surfaces. The carbon (bottom-right) and nitrogen (bottom-left) core level spectra of bare (black curves) and melamine-covered (red curves) Pt(111) surfaces indicate successful deposition of melamine. The schematic (inset, top) gives the structure of isolated melamine and the suggested structure of melamine adsorbed on Pt(111) based on stoichiometric analysis of nitrogen functionalities from the nitrogen core level spectrum for Pt(111)-M_{ad}.

spectra). Melamine is a heterocyclic aromatic molecule composed of a triazine ring (C_3N_3) with one amine group ($-NH_2$) bonded to each of the carbon atoms in the aromatic ring (inset on Fig. 2)⁴². Although the binding energies (BEs) of C=O and C-N (as well as C=O and C=N) bonds are very close to each other, making it difficult to uniquely fit the carbon core level spectra, an increase of carbon peak intensity at BE \sim 286–288 eV for Pt(111)-M_{ad} relative to unmodified Pt(111) points towards successful deposition of melamine on the platinum surface. Analysis of the nitrogen core level spectrum for Pt(111)-M_{ad} further indicates the presence of both N=C and $-NH_2$ functionalities at BEs 398.1 and 399.5 eV, respectively, consistent with the presence of melamine on the surface. In contrast, the nitrogen core level spectrum for unmodified Pt(111) shows no visible features, confirming that all nitrogen content present on Pt(111)-M_{ad} derives from the melamine assembly. Interestingly, N=C and $-NH_2$ functionalities on Pt(111)-M_{ad} surfaces are present in a ratio of \sim 2:3 instead of the 1:1 ratio expected for isolated melamine molecules. This deviation from the expected stoichiometry suggests that melamine molecules may be adsorbed via one of the cyclic carbon atoms, resulting in the release of an amine group (for proposed scheme please refer to inset in Fig. 2). Overall, the XPS results presented in this work are in accordance with previous papers found in literature,

where the high chemical integrity and robustness of melamine networks on metal surfaces was demonstrated under both atmospheric²⁰ and UHV conditions⁴³. We note in passing that we also performed an extensive STM investigation of the Pt(111)-M_{ad} surface and could not find an ordered melamine structure, suggesting that the melamine adlayer on Pt(111) is in fact disordered.

In order to make a reliable analysis of the ORR activities for the platinum surfaces described above, we will adopt the equation previously proposed in refs. ^{9,12}:

$$i_{E_x} = nFK_x c_{O_2} [1 - \Theta_{cov.}(\Delta G_{cov.-spec.}) - \Theta_{non-cov.}(\Delta G_{non-cov.-spec.})] \quad (1),$$

where i_{E_x} is the current density of a generic electrocatalyst (x) at a particular potential (here we will use $E_x = 0.9$ V for ORR kinetic analysis), n is the number of electrons transferred during the reduction of one mole of oxygen molecules, F is the Faraday constant, K_x is a constant, c_{O_2} is the concentration of oxygen molecules dissolved in the electrolyte solution, $\Theta_{cov.} + \Theta_{non-cov.} = \Theta_{ad}$ is the fraction of the electrode surface that is blocked by covalently and non-covalently adsorbed species,

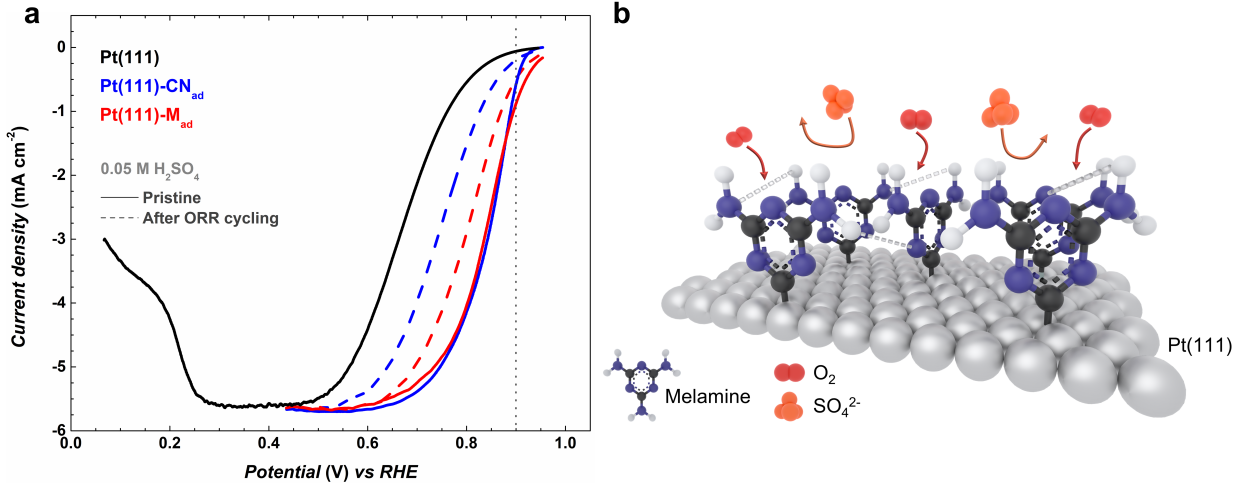


Figure 3. ORR polarization curves of the modified Pt(111) surfaces before and after extensive potential cycling excursions, and proposed model for selective adsorption of melamine molecules together with schematic presentation of the availability of platinum surface atoms for adsorption of O₂ molecules on Pt(111)-M_{ad}. **a**, The curves were measured in O₂-saturated 0.05 M sulfuric acid solutions (~293 K), at sweep rate of 50 mV s⁻¹, and 1,600 r.p.m. using the rotating disc electrode configuration. A dotted-vertical line is present as an eye-guide to spot the difference in ORR activities (E = 0.9 V) of the modified Pt(111) surfaces before (solid curves) and after several potential cycles (0.45 V > E > 0.95 V) (dashed curves). The bare Pt(111) ORR polarization curve (black curve) is also shown for comparison. **b**, The number of sites required for O₂ adsorption is significantly increased on the Pt(111)-M_{ad} surface because adsorption of (bi)sulfate anions is sterically suppressed by the formation of a “multi-dentate” (due to hydrogen-bonds) melamine adlayer.

and $\Delta G_{cov.-spec}$ and $\Delta G_{non-cov.-spec}$ are the free energy of the adsorption of their respective species (‘spectators’) on electrode surface. It is important to be aware that covalent bonding of spectator species on platinum and platinum-group metal surfaces depends strongly on the metal-spectator energetics ($\Delta G_{cov.-spec}$), hence the rate of reaction will be strongly related to the nature of the metal surface. Usually, the covalently-bound spectators relevant for ORR electrocatalysis are strongly adsorbing anions¹² (e.g., SO₄²⁻, HSO₄⁻, Cl⁻, and NO₃⁻, to name a few), OH_{ad} and H_{upd}, although in our case, CN_{ad} and M_{ad} must be also considered [please refer to Fig. 1a for the influence of cyanide, Pt(111)-CN_{ad}, and melamine, Pt(111)-M_{ad}, spectators on the overall CV profiles compared to the Pt(111) surface]. Although the extent of interaction between covalently bounded spectators and hydrated ions located at the double layer region (specifically, the outer Helmholtz phase, OHP) can also influence the reaction rate (i.e., current density i_{E_x})⁹, this phenomenon is less pronounced in acidic electrolytes free of foreign cations (e.g., Li⁺, Na⁺, K⁺, etc.). Therefore, the $\Theta_{non-cov}(\Delta G_{non-cov.-spec})$ term [Eq. (1)] will have a small influence on i_{E_x} in sulfuric acid electrolyte and can be neglected in this case.

Considering the approach described in the last paragraph for the activity analysis for ORR in acidic media, we start our discussion with the simplest solid/liquid interface employed in this work: the Pt(111) surface in contact with 0.05 M H₂SO₄ solution saturated with O₂ (Fig. 1b, black curve). Some general aspects of the electrocatalytic behavior must be assigned. First, poor activity at 0.85 V for the ORR is observed due to the strong adsorption of (bi)sulfate anions on Pt(111) surface⁴⁰, i.e. low availability of active sites or low $1 - \Theta_{cov}(\Delta G_{cov.-spec})$ [Eq. (1)]. A ORR polarization curve for Pt(111) in 0.1 M HClO₄ solution is also shown for comparison (Fig. 1b, gray dashed curve), as ClO₄⁻ is a well-known weakly-adsorbing anion¹². Second, oxygen reduction proceeds through a 4e⁻ reaction

pathway on Pt(111) in both acidic environments at potentials higher than 0.4 V despite the higher ORR activity in perchloric acid solution. Third, the formation of H_{upd} results in an ORR pathway change to a 2e⁻ route at E < 0.4 V^{12,40}. Finally, the intermediates formed during the ORR have a small contribution to the covered-amount of species on platinum surface, i.e. they have a minor contribution to the Θ_{ad} term in Eq. (1) and thus play a small role in controlling the ORR kinetics on platinum.

The CN_{ad} and M_{ad} platinum surfaces both show improved activity for oxygen reduction (Fig. 1b, blue and red curves, respectively) compared to the bare platinum surface: a factor of 22 higher for Pt(111)-CN_{ad} and a factor of 20 higher for Pt(111)-M_{ad} at E = 0.85 V. A notable difference between these modified surfaces is the change of the slope of the ORR curve above ~0.9 V. We attribute this feature to the contribution of OH_{ad} adsorption to the additional coverage on Pt(111)-CN_{ad}⁸ (see cyclic voltammetry for this surface at Fig. 1a, blue curve) hence reducing the activity for the ORR. As for Pt(111)-M_{ad}, the ORR curve at E > 0.9 V in 0.05 M H₂SO₄ matches the one for Pt(111) in 0.1 M HClO₄ (both CV and ORR curves for Pt(111)-M_{ad} in 0.1 M HClO₄, along with Pt(111)’s respective curves for comparison, can be found in Supplemental Information, Fig. S1). This is a first sign that M_{ad} does not contribute to suppressing the Pt(111) ORR activity in the kinetically controlled potential region. Indeed, the activity of Pt(111)-M_{ad} is a factor of 1.6 higher than that of Pt(111)-CN_{ad} for ORR at E = 0.9 V⁴⁰. We also note that a 4e⁻ pathway for oxygen reduction is observed on both modified platinum surfaces, which implies that CN_{ad} and M_{ad} do not influence the ORR mechanism^{8,9,12,40}. Therefore, we can assume that CN_{ad} and M_{ad} adlayers act purely as a steric blockage, implying that the kinetics for ORR must be governed purely by the $(1 - \Theta_{ad})$ term in Eq. (1).

Despite the significant improvement in ORR activity by the modified platinum surfaces, it is also important to consider the stability of these electrocatalysts at relevant potential values. For ORR catalysts, stability between 0.6 V and 0.95 V is often

needed. Fig. 3 shows the ORR polarization curves for pristine and cycled (0.4 V < E < 0.95 V) Pt(111)-CN_{ad} and Pt(111)-M_{ad} surfaces [pristine Pt(111) is also shown for comparison]. Both ‘aged’ ORR polarization curves for the two modified surfaces shown in Fig. 3 were obtained after their ORR activity stabilized during the potential cycling (100 cycles between 0.4 V < E < 0.95 V). Both modified platinum surfaces remain more active towards the ORR than Pt(111), with Pt(111)-M_{ad} and -CN_{ad} surfaces exhibiting a factor of 9 and 3 higher activity, respectively, than bare Pt(111). The reason for the Pt(111)-M_{ad} and Pt(111)-CN_{ad} interface instability, and thus their partial deactivation, is most likely result of M_{ad}/CN_{ad} oxidation or displacement through (bi)sulfate or OH_{ad} adsorption. More importantly though, the Pt(111)-M_{ad} shows a much higher stability than Pt(111)-CN_{ad}, resulting in a 75 mV lower overpotential for the ORR. As mentioned earlier, the purpose of chemical modification with melamine, as opposed to cyanide, was to create the possibility of a stronger adsorption of the molecules to the catalyst surface, either through strengthening the single bond or creating a multi-dentate bonding to the surface by taking advantage of the intermolecular networks formed by hydrogen-bonds for various metal-melamine systems, previously demonstrated in other studies. While the XPS results suggest melamine adsorption through a release of an amine group, they do not supply structural information about the melamine adlayer or its binding to the surface. However, it seems that the vertical orientation of the molecules might be the most plausible, as depicted in Figure 3b. While strengthening of the single bond between melamine and Pt is possible, compared to Pt-CN, it is highly likely that the melamine network is constructed through intermolecular hydrogen-bonds formed by the -NH₂ groups (proton donors through their hydrogen atoms) and the nitrogen atoms in the C₃N₃ heterocycle (proton acceptors through their isolated pair of electrons)^{20,42}. Although the energy of a hydrogen-bond (order of ~33 kJ mol⁻¹ for a two-fold hydrogen-bond) is not strong relative to a coordination bond type (~62 kJ mol⁻¹), previous works had showed the formation of highly ordered, hydrogen-bonded melamine networks on various metal substrates (in part also due to the planar geometry and aromaticity of melamine molecules)^{16,20,42,43}. This intermolecular hydrogen-bonded adlayer of melamine was found to have remarkable structural stability, being able to be analyzed even in a liquid/solid interface by scanning tunneling microscopy (STM)¹⁶. Therefore, it is reasonable to consider that the melamine adlayer consists of multiple hydrogen-bonded macromolecular entities with multiple bonds attaching them to the Pt surface, which in turn promotes the stability of the Pt(111)-M_{ad} surface for the ORR when compared to the Pt(111)-CN_{ad} surface.

CONCLUSIONS

We produced a molecular adlayer of melamine on Pt(111) surface [Pt(111)-M_{ad}] through a simple drop-casting method to enhance the Pt(111) activity for ORR in highly adsorbing electrolytes. The Pt(111)-M_{ad} presented a >20-fold increase of the ORR activity at E = 0.85 V, which is comparable to the ~22-fold increase obtained for the Pt(111)-CN_{ad}, known from our previous work⁸. We rationalize that M_{ad} moieties on Pt(111) surface, as for CN_{ad}, can successfully block the Pt(111) surface active sites from adsorption of poisonous spectator species such as (bi)sulfate anions without compromising the adsorption of O₂ or the 4e⁻ mechanism of the ORR observed on the bare Pt(111) surface. Moreover, unlike the CN_{ad}, M_{ad} moieties also suppress the OH_{ad} adsorption, resulting in a slightly higher activity of

Pt(111)-M_{ad} interface at E = 0.9 V compared to Pt(111)-CN_{ad} interface. Furthermore, under the same electrochemical conditions, the Pt(111)-M_{ad} surface is strikingly more stable than the Pt(111)-CN_{ad} surface [retaining an activity improvement factor higher than 9 and 3 for ORR activity in Pt(111)-M_{ad} and Pt(111)-CN_{ad}, respectively, compared to the bare Pt(111), after potential cycling]. We propose the intermolecular hydrogen-bonding in the melamine networks as the ‘stability promoter’ for the Pt(111)-M_{ad} interfaces, creating an adlayer of multi-dentate macromolecules. Although the results showed in this work are concentrated on the single-crystalline Pt(111) surface, the fundamental principles of chemical modification of electrocatalytic surfaces to achieve a higher activity, stability, and selectivity are broadly applicable to other solid/liquid interfaces for energy conversion and storage applications.

AUTHOR INFORMATION

Corresponding Author

* E-mail: strmcnik@anl.gov

Author Contributions

The manuscript was written through contributions of all authors. All authors have given approval to the final version of the manuscript.

ACKNOWLEDGMENT

The research was supported by the Office of Science, Office of Basic Energy Sciences, Materials Sciences and Engineering Division, and was carried out at Argonne National Laboratory which is supported by the U.S. Department of Energy, Office of Science, Office of Basic Energy Sciences, under Contract No. DE-AC02-06CH1135. The authors thank Francisco S. Dias Martins Jr. for assisting the preparation of the artwork shown in this work.

REFERENCES

- (1) Kulkarni, A.; Siahrostami, S.; Patel, A.; Nørskov, J. K. Understanding Catalytic Activity Trends in the Oxygen Reduction Reaction. *Chem. Rev.* **2018**, *118* (5), 2302–2312. <https://doi.org/10.1021/acs.chemrev.7b00488>.
- (2) Jiao, Y.; Zheng, Y.; Jaroniec, M.; Qiao, S. Z. Design of Electrocatalysts for Oxygen- and Hydrogen-Involving Energy Conversion Reactions. *Chem. Soc. Rev.* **2015**, *44* (8), 2060–2086. <https://doi.org/10.1039/C4CS00470A>.
- (3) Shao, M.; Chang, Q.; Dodelet, J.-P.; Chenitz, R. Recent Advances in Electrocatalysts for Oxygen Reduction Reaction. *Chem. Rev.* **2016**, *116* (6), 3594–3657. <https://doi.org/10.1021/acs.chemrev.5b00462>.
- (4) Wang, C.; Markovic, N. M.; Stamenkovic, V. R. Advanced Platinum Alloy Electrocatalysts for the Oxygen Reduction Reaction. *ACS Catal.* **2012**, *2* (5), 891–898. <https://doi.org/10.1021/cs3000792>.
- (5) Katsounaros, I.; Cherevko, S.; Zeradjanin, A. R.; Mayrhofer, K. J. J. Oxygen Electrochemistry as a Cornerstone for Sustainable Energy Conversion. *Angew. Chemie Int. Ed.* **2014**, *53* (1), 102–121. <https://doi.org/10.1002/anie.201306588>.
- (6) Greeley, J.; Stephens, I. E. L.; Bondarenko, A. S.; Johansson, T. P.; Hansen, H. A.; Jaramillo, T. F.; Rossmeisl, J.; Chorkendorff, I.; Nørskov, J. K. Alloys of Platinum and Early Transition Metals as Oxygen Reduction Electrocatalysts. *Nat. Chem.* **2009**, *1*, 552.
- (7) Strasser, P.; Koh, S.; Anniyev, T.; Greeley, J.; More, K.; Yu, C.; Liu, Z.; Kaya, S.; Nordlund, D.; Ogasawara, H.; Toney, M. F.; Nilsson, A. Lattice-Strain Control of the Activity in Dealloyed Core–Shell Fuel Cell Catalysts. *Nat. Chem.* **2010**, *2* (6), 454–460. <https://doi.org/10.1038/nchem.623>.
- (8) Strmcnik, D.; Escudero-Escribano, M.; Kodama, K.; Stamenkovic, V. R.; Cuesta, A.; Marković, N. M. Enhanced Electrocatalysis of the Oxygen Reduction Reaction Based on Patterning of Platinum Surfaces with Cyanide. *Nat. Chem.* **2010**,

(9) 2, 880.
Strmcnik, D.; Kodama, K.; van der Vliet, D.; Greeley, J.; Stamenkovic, V. R.; Marković, N. M. The Role of Non-Covalent Interactions in Electrocatalytic Fuel-Cell Reactions on Platinum. *Nat. Chem.* **2009**, *1*, 466.

(10) Li, G.-F.; Divinagracia, M.; Labata, M. F.; Ocon, J. D.; Abel Chuang, P.-Y. Electrolyte-Dependent Oxygen Evolution Reactions in Alkaline Media: Electrical Double Layer and Interfacial Interactions. *ACS Appl. Mater. Interfaces* **2019**, *11* (37), 33748–33758. <https://doi.org/10.1021/acsami.9b06889>.

(11) Damjanovic, A.; Genshaw, M. A.; Bockris, J. O. Distinction between Intermediates Produced in Main and Side Electrode Reactions. *J. Chem. Phys.* **1966**, *45* (11), 4057–4059. <https://doi.org/10.1063/1.1727457>.

(12) Marković, N. M.; Ross, P. N. Surface Science Studies of Model Fuel Cell Electrocatalysts. *Surf. Sci. Rep.* **2002**, *45* (4), 117–229. [https://doi.org/https://doi.org/10.1016/S0167-5729\(01\)00022-X](https://doi.org/https://doi.org/10.1016/S0167-5729(01)00022-X).

(13) Cuesta, A. At Least Three Contiguous Atoms Are Necessary for CO Formation during Methanol Electrooxidation on Platinum. *J. Am. Chem. Soc.* **2006**, *128* (41), 13332–13333. <https://doi.org/10.1021/ja0644172>.

(14) Cuesta, A.; Escudero, M.; Lanova, B.; Baltruschat, H. Cyclic Voltammetry, FTIRs, and DEMS Study of the Electrooxidation of Carbon Monoxide, Formic Acid, and Methanol on Cyanide-Modified Pt(111) Electrodes. *Langmuir* **2009**, *25* (11), 6500–6507. <https://doi.org/10.1021/la8041154>.

(15) Stamenkovic, V. R.; Strmcnik, D.; Lopes, P. P.; Markovic, N. M. Energy and Fuels from Electrochemical Interfaces. *Nat. Mater.* **2016**, *16*, 57.

(16) Uemura, S.; Aono, M.; Komatsu, T.; Kunitake, M. Two-Dimensional Self-Assembled Structures of Melamine and Melem at the Aqueous Solution–Au(111) Interface. *Langmuir* **2011**, *27* (4), 1336–1340. <https://doi.org/10.1021/la103948n>.

(17) Lin, Y.-P.; Ourdjini, O.; Giovanelli, L.; Clair, S.; Faury, T.; Ksari, Y.; Themlin, J.-M.; Porte, L.; Abel, M. Self-Assembled Melamine Monolayer on Cu(111). *J. Phys. Chem. C* **2013**, *117* (19), 9895–9902. <https://doi.org/10.1021/jp401496s>.

(18) Greenwood, J.; Früchtl, H. A.; Baddeley, C. J. Ordered Growth of Upright Melamine Species on Ni{111}: A Study with Scanning Tunnelling Microscopy and Reflection Absorption Infrared Spectroscopy. *J. Phys. Chem. C* **2012**, *116* (11), 6685–6690. <https://doi.org/10.1021/jp212055u>.

(19) Greenwood, J.; Früchtl, H. A.; Baddeley, C. J. Self-Assembly of Upright, Partially Dehydrogenated Melamine on Pd(111). *J. Phys. Chem. C* **2013**, *117* (44), 22874–22879. <https://doi.org/10.1021/jp407303e>.

(20) Zhu, L.; Xu, X.; Wang, Y.; Liu, S.; Ling, J.; Liu, L.; Wei, S.; Cai, F.; Wang, Z.; Liu, X.; Wang, L. Hydrogen-Bonded Structures of Trimesic and Melamine on Highly Oriented Pyrolytic Graphite. *Surf. Rev. Lett.* **2014**, *21* (03), 1450035. <https://doi.org/10.1142/S0218625X14500358>.

(21) Asahi, M.; Yamazaki, S.; Taguchi, N.; Ioroi, T. Facile Approach to Enhance Oxygen Reduction Activity by Modification of Platinum Nanoparticles by Melamine-Formaldehyde Polymer. *J. Electrochem. Soc.* **2019**, *166* (8), F498–F505. <https://doi.org/10.1149/2.0641908jes>.

(22) Wada, N.; Nakamura, M.; Hoshi, N. Structural Effects on the Oxygen Reduction Reaction on Pt Single-Crystal Electrodes Modified with Melamine. *Electrocatalysis* **2020**, *11* (3), 275–281. <https://doi.org/10.1007/s12678-020-00584-0>.

(23) Genorio, B.; Strmcnik, D.; Subbaraman, R.; Tripkovic, D.; Karapetrov, G.; Stamenkovic, V. R.; Pejovnik, S.; Marković, N. M. Selective Catalysts for the Hydrogen Oxidation and Oxygen Reduction Reactions by Patterning of Platinum with Calix[4]Arene Molecules. *Nat. Mater.* **2010**, *9* (12), 998–1003. <https://doi.org/10.1038/nmat2883>.

(24) Subbaraman, R.; Tripkovic, D.; Chang, K.-C.; Strmcnik, D.; Paulikas, A. P.; Hirunsit, P.; Chan, M.; Greeley, J.; Stamenkovic, V.; Markovic, N. M. Trends in Activity for the Water Electrolyser Reactions on 3d M(Ni,Co,Fe,Mn) Hydr(Oxy)Oxide Catalysts. *Nat. Mater.* **2012**, *11* (6), 550–557. <https://doi.org/10.1038/nmat3313>.

(25) Subbaraman, R.; Tripkovic, D.; Strmcnik, D.; Chang, K.-C.; Uchimura, M.; Paulikas, A. P.; Stamenkovic, V.; Markovic, N. M. Enhancing Hydrogen Evolution Activity in Water Splitting by Tailoring Li+-Ni(OH)2-Pt Interfaces. *Science (80-.).* **2011**, *334* (6060), 1256–1260. <https://doi.org/10.1126/science.1211934>.

(26) Strmcnik, D. S.; Tripkovic, D. V.; van der Vliet, D.; Chang, K.-C.; Komanicky, V.; You, H.; Karapetrov, G.; Greeley, J. P.; Stamenkovic, V. R.; Marković, N. M. Unique Activity of Platinum Adislands in the CO Electrooxidation Reaction. *J. Am. Chem. Soc.* **2008**, *130* (46), 15332–15339. <https://doi.org/10.1021/ja8032185>.

(27) Walton, J.; Wincott, P.; Fairley, N.; Carrick, A. *Peak Fitting with CasaXPS: A Casa Pocket Book*; Accolyte Science: United Kingdom, 2010.

(28) Kim, Y.-G.; Yau, S.-L.; Itaya, K. Direct Observation of Complexation of Alkali Cations on Cyanide-Modified Pt(111) by Scanning Tunneling Microscopy. *J. Am. Chem. Soc.* **1996**, *118* (2), 393–400. <https://doi.org/10.1021/ja9521841>.

(29) Stickney, J. L.; Rosasco, S. D.; Salaita, G. N.; Hubbard, A. T. Ordered Ionic Layers Formed on Platinum(111) from Aqueous Solutions. *Langmuir* **1985**, *1* (1), 66–71. <https://doi.org/10.1021/la00061a009>.

(30) Huerta, F. J.; Morallón, E.; Vazquez, J.; Aldaz, A. Voltammetric and Spectroscopic Characterization of Cyanide Adlayers on Pt(h,k,l) in an Acidic Medium. *Surf. Sci.* **1998**, *396* (1), 400–410. [https://doi.org/https://doi.org/10.1016/S0039-6028\(97\)00694-8](https://doi.org/https://doi.org/10.1016/S0039-6028(97)00694-8).

(31) Stuhlmann, C. Characterization of an Electrode Adlayer by In-Situ Infrared Spectroscopy: Cyanide on Pt(111). *Surf. Sci.* **1995**, *335*, 221–226. [https://doi.org/https://doi.org/10.1016/0039-6028\(95\)00420-3](https://doi.org/https://doi.org/10.1016/0039-6028(95)00420-3).

(32) Friedrich, K. A.; Daum, W.; Klünker, C.; Knabben, D.; Stimming, U.; Ibach, H. In-Situ Spectroscopy of Cyanide Vibrations on Pt(111) and Pt(110) Electrode Surfaces: Potential Dependencies and the Influence of Surface Disorder. *Surf. Sci.* **1995**, *335*, 315–325. [https://doi.org/https://doi.org/10.1016/0039-6028\(95\)00579-X](https://doi.org/https://doi.org/10.1016/0039-6028(95)00579-X).

(33) Schardt, B. C.; Stickney, J. L.; Stern, D. A.; Frank, D. G.; Katekaru, J. Y.; Rosasco, S. D.; Salaita, G. N.; Soriaga, M. P.; Hubbard, A. T. Surface Coordination Chemistry of Well-Defined Platinum Electrodes: Surface Polyprotic Acidity of Platinum(111)(2 ∙ Sqroot. 3 ∙ Times. 2 ∙ Sqroot. 3)R30.Degree.-Hydrogen Isocyanide. *Inorg. Chem.* **1985**, *24* (10), 1419–1421. <https://doi.org/10.1021/ic00204a001>.

(34) Frank, D. G.; Katekaru, J. Y.; Rosasco, S. D.; Salaita, G. N.; Schardt, B. C.; Soriaga, M. P.; Stern, D. A.; Stickney, J. L.; Hubbard, A. T. PH and Potential Dependence of the Electrical Double Layer at Well-Defined Electrode Surfaces: Cs+ and Ca2+ Ions at Pt(111) (2√3 X 2√3)R30°-CN, Pt(111) (√13 X √13)R14°-CN, and Pt(111) (2 X 2)-SCN. *Langmuir* **1985**, *1* (5), 587–592. <https://doi.org/10.1021/la00065a013>.

(35) Huerta, F.; Morallón, E.; Quijada, C.; Vázquez, J. L.; Berlouis, L. E. A. Potential Modulated Reflectance Spectroscopy of Pt(111) in Acidic and Alkaline Media: Cyanide Adsorption. *J. Electroanal. Chem.* **1999**, *463* (1), 109–115. [https://doi.org/https://doi.org/10.1016/S0022-0728\(98\)00453-7](https://doi.org/https://doi.org/10.1016/S0022-0728(98)00453-7).

(36) Huerta, F.; Morallón, E.; Quijada, C.; Vázquez, J. L.; Aldaz, A. Spectroelectrochemical Study on CN- Adsorbed at Pt(111) in Sulphuric and Perchloric Media. *Electrochim. Acta* **1998**, *44* (6), 943–948. [https://doi.org/https://doi.org/10.1016/S0013-4686\(98\)00197-2](https://doi.org/https://doi.org/10.1016/S0013-4686(98)00197-2).

(37) Huerta, F.; Morallón, E.; Vázquez, J. L. Structural Effects of Adsorbed CN Adlayers on the Co-Adsorption of OH- at the Pt(111) Surface in Sulfuric Acid Medium. *Surf. Sci.* **1999**, *431* (1), L577–L581. [https://doi.org/https://doi.org/10.1016/S0039-6028\(99\)00580-4](https://doi.org/https://doi.org/10.1016/S0039-6028(99)00580-4).

(38) Inukai, J.; Morioka, Y.; Kim, Y.-G.; Yau, S.-L.; Itaya, K. Cation Effects on Infrared Reflection Absorption Spectra of Cyanide Adsorbed on Pt(111) Electrode in Electrolyte Solutions. *Bull. Chem. Soc. Jpn.* **1997**, *70* (8), 1787–1794. <https://doi.org/10.1246/bcsj.70.1787>.

(39) Kim, C. S.; Korzeniewski, C. Cyanide Adsorbed as a Monolayer at the Low-Index Surface Planes of Platinum Metal Electrodes: An in Situ Study by Infrared Spectroscopy. *J. Phys. Chem.* **1993**, *97* (38), 9784–9787. <https://doi.org/10.1021/j100140a041>.

(40) Markovic, N. M.; Gasteiger, H. A.; Ross, P. N. Oxygen Reduction on Platinum Low-Index Single-Crystal Surfaces in Sulfuric Acid Solution: Rotating Ring-Pt(Hkl) Disk Studies. *J. Phys. Chem.* **1995**, *99* (11), 3411–3415. <https://doi.org/10.1021/j100011a001>.

(41) Wang, J. X.; Markovic, N. M.; Adzic, R. R. Kinetic Analysis of Oxygen Reduction on Pt(111) in Acid Solutions: Intrinsic Kinetic Parameters and Anion Adsorption Effects. *J. Phys. Chem. B* **2004**, *108* (13), 4127–4133. <https://doi.org/10.1021/jp037593v>.

(42) Walch, H.; Maier, A.-K.; Heckl, W. M.; Lackinger, M. Isotopological Supramolecular Networks from Melamine and Fatty Acids. *J. Phys. Chem. C* **2009**, *113* (3), 1014–1019.

(43) <https://doi.org/10.1021/jp8078474>.
Silly, F.; Shaw, A. Q.; Castell, M. R.; Briggs, G. A. D.; Mura, M.; Martsinovich, N.; Kantorovich, L. Melamine Structures on the Au(111) Surface. *J. Phys. Chem. C* **2008**, *112* (30), 11476–11480. <https://doi.org/10.1021/jp8033769>.

Table of Contents artwork:

